DRAFT VERSION FEBRUARY 4, 2021
Typeset using LaTeX **twocolumn** style in AASTeX62

The nature of the eccentric doubled-lined eclipsing binary system KIC 2306740 with *Kepler* space photometry

D. KOÇAK,[1] K. YAKUT,[1,2] J. SOUTHWORTH,[3] P. P. EGGLETON,[4] T. İÇLI,[1] C. A. TOUT,[2] AND S. BLOEMEN[5,6]

[1]*Department of Astronomy and Space Sciences, University of Ege, 35100, Bornova–İzmir, Turkey*
[2]*Institute of Astronomy, University of Cambridge, Madingley Road, Cambridge CB3 0HA, UK*
[3]*Astrophysics Group, Keele University, Staffordshire ST5 5BG, UK*
[4]*Lawrence Livermore National Laboratory, 7000 East Ave, Livermore, CA94551, USA*
[5]*Instituut voor Sterrenkunde, Katholieke Universiteit Leuven, Celestijnenlaan 200D, B-3001 Leuven, Belgium*
[6]*Department of Astrophysics, IMAPP, University of Nijmegen, PO Box 9010, 6500 GL Nijmegen,, the Netherlands*

(Received February 4, 2021; Revised February 4, 2021; Accepted February 4, 2021)

Submitted to ApJ

ABSTRACT

We present a detailed study of KIC 2306740, an eccentric double-lined eclipsing binary system. *Kepler* satellite data were combined with spectroscopic data obtained with the 4.2 m William Herschel Telescope (WHT). This allowed us to determine precise orbital and physical parameters of this relatively long period ($P = 10\overset{\mathrm{d}}{.}3$) and slightly eccentric, ($e = 0.3$) binary system. The physical parameters have been determined as $M_1 = 1.194 \pm 0.008\,\mathrm{M}_\odot$, $M_2 = 1.078 \pm 0.007\,\mathrm{M}_\odot$, $R_1 = 1.682 \pm 0.004\,\mathrm{R}_\odot$, $R_2 = 1.226 \pm 0.005\,\mathrm{R}_\odot$, $L_1 = 2.8 \pm 0.4\,\mathrm{L}_\odot$, $L_2 = 1.8 \pm 0.2\,\mathrm{L}_\odot$ and orbital seperation $a = 26.20 \pm 0.04\,\mathrm{R}_\odot$ through simultaneous solutions of *Kepler* light curves and of the WHT radial velocity data. Binarity effects were extracted from the light curve in order to study intrinsic variations in the residuals. Five significant and more than 100 combination frequencies were detected. We modeled the binary system assuming non-conservative evolution models with the Cambridge STARS (TWIN) code and we show evolutionary tracks of the components in the $\log L - \log T$ plane, the $\log R - \log M$ plane and the $\log P - \mathrm{age}$ plane for both spin and orbital periods together with eccentricity e and $\log R_1$. The model of the non-conservative processes in the code led the system to evolve to the observed system parameters in roughly 5.1 Gyr.

Keywords: stars: evolution — stars: binaries: eclipsing — stars: binaries: spectroscopic — stars: oscillations — stars: individual: KIC 2306740

1. INTRODUCTION

Double-lined eclipsing detached binary stars are an important source for accurately determining the physical parameters of the component stars (Torres, Andersen, & Giménez 2010). Pulsations can be used for determining physical parameters as well as understanding stellar structure. Pulsating components in binary systems play an important role in understanding stellar structure because they are effectively laboratories for investigating stellar interiors (Aerts 2013).Therefore, having a pulsating component in a binary provides an independed verification of stellar parameters. Using continuous high precision observations from the CoRoT, *Kepler* and TESS satellites' data provide the opportunity to study a variety of pulsating stars in binary systems. Recently many observational results for different type pulsating stars, including those of binary components, have been studied in the literature (e.g. Wood, Olivier & Kawaler 2004; Yakut, Aerts & Morel 2007; Welsh, et al. 2011; Maceroni et al. 2014; Murphy, Moe, Kurtz, Bedding, Shibahashi & Boffin 2018; Qian, Li, He, Zhang, Zhu & Han 2018; Johnston, et al. 2019). Pulsating stars in close binary systems have been discussed in detail by many authors (e.g. Zahn 1975; Aerts & Harmanec 2004; Breger 2005; Reed, Brondel & Kawaler 2005; Aerts, Christensen-Dalsgaard, & Kurtz 2010; Huber 2015; Southworth et al. 2020).

The *Kepler* satellite observed more than 200,000 stars, including some with planetary companions, binary/multiple stellar systems, and pulsating stars, to obtain very high precision photometry (Koch et al. 2010; Borucki et al. 2010; Gilliland et al. 2010; Brown et al. 2011).These photometric results have found previously unknown variations, providing further constraints to current models. The precision of the *Kepler* observations allow us to disentangle low-amplitude variation in a binary star system. One such system is KIC 2306740 which will be the focus of this work.

Table 1. Basic parameters for KIC 2306740. B and V color values are taken from Zacharias et al. (2005) and other parameters are taken from the Kepler Input Catalogue, Gaia and Simbad.

Parameter	Value
2MASS ID	19290475+3741535
Gaia ID	2051885033280089216
α_{2000}	19 29 04.75
δ_{2000}	+37 41 53.5
B	$13\overset{\mathrm{m}}{.}91$
V	$13\overset{\mathrm{m}}{.}08$
R	$12\overset{\mathrm{m}}{.}92$
G (Gaia)	$13\overset{\mathrm{m}}{.}473$
J (2MASS)	$12\overset{\mathrm{m}}{.}297$
H (2MASS)	$12\overset{\mathrm{m}}{.}022$
K_s(2MASS)	$11\overset{\mathrm{m}}{.}958$
K_p(*Kepler*)	$13\overset{\mathrm{m}}{.}545$
E_{B-V}	$0\overset{\mathrm{m}}{.}117$
Period	10.31 d
π (mas)	0.6606

KIC 2306740 ($P = 10\overset{\mathrm{d}}{.}3$, $e = 0.3$, V=$13\overset{\mathrm{m}}{.}08$, $K_p = 13\overset{\mathrm{m}}{.}55$) is an eccentric double-lined detached eclipsing binary system that was discovered by *Kepler* satellite. Some basic parameters for the system given in Table 1. The first preliminary binary solution of the system was found by Prša et al. (2011). They refined the orbital period as $10\overset{\mathrm{d}}{.}30399 \pm 0\overset{\mathrm{d}}{.}00003$ and temperature ratio ($T_2/T1$) as 0.834. Kjurkchieva, Vasileva, & Atanasova (2017) subsequently estimated the relative radii of the components as $r_1 = 0.0.612$ and $r_2 = 0.0600$, mass ratio as 0.972, the orbital eccentricity as 0.299, and the argument of periastron as 275°. However, the parameters obtained in the current work are quite different from those two studies. This is because of the careful interactive analysis of the light curve (LC) and radial velocity (RV) data made in this study, rather than the automated LC modeling.

In this paper we study the binary nature of the system as well its and rotational behaviour using the *Kepler* data combined with a set of high precision RVs. KIC 2306740 was observed by *Kepler* in quarters Q0 to Q16. The new spectroscopic observations and data analysis of radial velocities are described in Section 2. We present the *Kepler* data and light curve solution of the system in Section 3. Using the radial velocity and light curve solution we obtained the physical parameters of the system in Section 4. Light variation outside eclipses is discussed in Section 5. Section 6 contains a discussion of the possible evolutionary state of the system and our conclusions.

2. SPECTROSCOPIC OBSERVATIONS

Table 2. Radial velocity measurements for KIC 2306740.

HJD (2456000+)	Phase	V_1 km s^{-1}	$(O-C)_1$ km s^{-1}	V_2 km s^{-1}	$(O-C)_2$ km s^{-1}
87.53965	0.76260	71.76	1.98	-39.20	1.98
87.62467	0.77085	71.16	2.91	-36.82	2.91
87.70422	0.77857	67.24	0.46	-37.60	0.46
88.48349	0.85417	51.19	0.08	-16.19	0.08
88.57612	0.86316	48.36	-0.81	-15.99	-0.81
88.70547	0.87571	45.49	-0.95	-12.52	-0.95
91.52893	0.14965	-13.81	-1.63	55.10	-1.63
91.58456	0.15504	-17.25	-4.00	56.01	-4.00
91.63997	0.16042	-16.16	-1.85	60.03	-1.85
92.53903	0.24765	-32.60	-2.67	77.83	-2.67
92.59339	0.25292	-35.81	-5.08	77.17	-5.08
92.65527	0.25893	-36.34	-4.73	78.21	-4.73
92.71038	0.26427	-36.34	-3.97	79.82	-3.97

We obtained spectra of KIC 2306740 at 15 epochs with the Intermediate dispersion Spectrograph and Imaging System (ISIS) on the William Herschel Telescope (WHT), in July 2012. These were timed to provide the best possible coverage of the orbital phases, given that the orbital period of 10.3 d is significantly longer than the duration of the observing run of 7 nights. Two epochs occurred close to eclipse when the velocity separation of the stars was small. These measured radial velocities are strongly affected by line blending and so were not used in our analysis.

WHT equipped with the double-armed ISIS. Spectra were taken simultaneously in the blue and red arms, covering the regions around Hγ and Hα. In the blue arm we used the grating H2400B, with a wavelength coverage of 4200 to 4550 Å. In the red arm the R1200R grating was used and gave coverage of 6100 to 6730 Å. The slit was set to 0.5 arcsec in order to limit the effects of telescope pointing errors so that a resolving power of $R \approx 22\,000$ is achieved. We used exposure times of 1500 s for all spectra to give a signal-to-noise (S/N) of roughly 30 per resolution element in the blue and 80 in the red. We bracketed each with spectra of CuAr+CuNe arc lamps for wavelength calibration. The data were reduced using the PAMELA package (Marsh 1989).

To measure the radial velocities (RVs) of the two stars from these spectra we used standard cross-correlation (e.g. Tonry & Davis 1979) and its two-dimensional extension TODCOR (Zucker & Mazeh 1994). Synthetic template spectra were calculated with the UCLSYN code (Smith 1992; Smalley et al. 2001) and ATLAS9 model atmospheres for metallicity, with a $T_{\rm eff}$ of 5500 K and no rotational broadening. For our final RVs we adopt those given by standard cross-correlation. These are very similar to those obtained with TODCOR.

Table 3. Spectroscopic orbital parameters of KIC 2306740. The standard errors σ are given in parentheses in the last digit quoted.

Parameter	e not fixed	e fixed at 0.301
T_0/d	2456399.19(24)	2456399.21(25)
P/d	10.3069(78)	10.3075(81)
e	0.322(22)	0.301
ω/rad	4.81(3)	4.80(3)
K_1/km s^{-1}	65.78(79)	63.98(76)
K_2/km s^{-1}	72.84(87)	70.86(84)
V_o/km s^{-1}	18.6(2)	18.6(2)
q = m_1/m_2	1.1073(90)	1.1074(88)
$a_1 \sin i/R_\odot$	12.682	12.425
$a_2 \sin i/R_\odot$	14.043	13.761
$m_1 \sin^3 i/M_\odot$	1.304	1.193
$m_2 \sin^3 i/M_\odot$	1.178	1.077

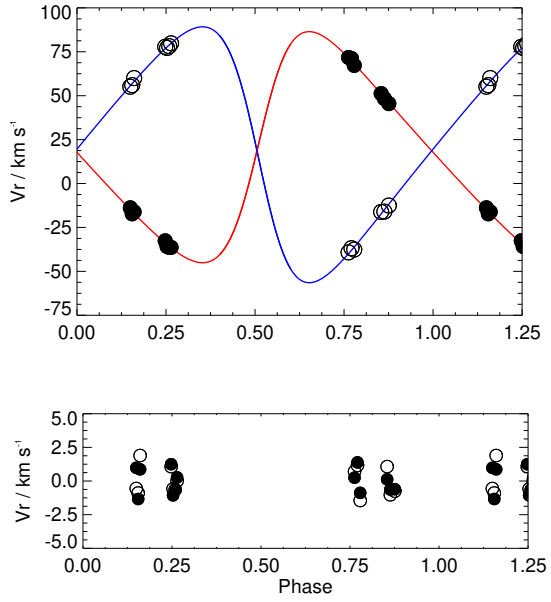

Figure 1. The radial velocity observations of KIC 2306740 as a function of phase. The filled and open circles represent the velocities of the primary and the secondary component, respectively. The residuals are shown in the bottom panel. The data are listed in Table 2 and the curve fitting corresponds to the elements given in Table 3.

3. *KEPLER* OBSERVATIONS OF THE SYSTEM AND MODELING OF THE LIGHT CURVE

The system was observed over approximately 1460 days during seventeen quarters (Q0 to Q16) with a long cadence (exposure time of about 30 min) and a total of 64 370 data points were obtained using the satellite. The light curve shows deep eclipses with periods of totality, plus periodic variations due to pulsations. *Kepler* satellite observations show some fluctuations due to common instrumental effects (Jenkins et al. 2010). Using the techniques outlined in (Jenkins et al. 2010), cotrending and detrending were applied to eliminate systematic variations. We studied each quarter separately and, to de-trend the data, a third-order polynomial fit was applied as we did in our earlier *Kepler* study (Yakut et al. 2015; Çokluk, et al. 2019). The raw data of KIC 2306740 is shown in Fig. 2 (upper panel). The de-trended normalized light variation is shown in Fig. 2 (lower panel). The quarters are shown in different colors.

Using the *Kepler* observations we derived the linear ephemeris given in Eq.1.

$$\text{HJD Min I} = 24\ 56399^{\text{d}}.1227(2) + 10^{\text{d}}.306988(2). \quad (1)$$

During the calculation of the orbital phases in the Figures 2 - 3 and Table 4 we used Eq.1.

The *Kepler* light curves along with the WHT RV curves were modeled simultaneously with the JKTEBOP code[1] (see Southworth, Maxted & Smalley 2004; Southworth 2013) and also with the PHOEBE (Prša & Zwitter 2005) program which uses the W–D code (Wilson and Devinney 1971). The curve dependent weights were assigned as described by Wilson (1979). We ran the code assuming a detached configuration. During analysis we iteratively solved the LC and RV curves: the LC gave a more accurate estimate of the eccentricity (0.30 ± 0.01) than did the RV curves (0.32 ± 0.02), and so we fixed e to this photometric solution when re-solving the RV curves. Even though *Kepler* data are very sensitive they are all obtained in a single filter. This prevents us from determining accurate temperatures from multiple color analyses. Since the spectral data obtain is not sufficient to determine a precise temperature, the temperature of the hotter star was fixed to 6060 K found in Armstrong et al. (2014).

To determine the uncertainties of the measured properties of the KIC 2306740 system, we turned to JKTEBOP as it is much faster than PHOEBE. JKTEBOP and derivatives of the Wilson-Devinney code have been found to yield results consistent at the 0.2% level or better in well-separated systems (Maxted, et al. 2020). For computational efficiency we phase-binned the data by sorting it into orbital phase and combining each group of 20 consecutive datapoints, giving a total of 3219 datapoints.

The phase-binned data and the radial velocities were modeled using JKTEBOP. The fitted parameters were the fractional radii, orbital eccentricity, inclination, argument of periastron, central surface brightness ratio of the stars, third light, the linear limb darkening coefficient of the primary star, and the velocity amplitude of each star and systemic velocity of the system. Limb darkening was implemented using the quadratic law for both stars. Numerical integra-

[1] http://www.astro.keele.ac.uk/jkt/codes/jktebop.html

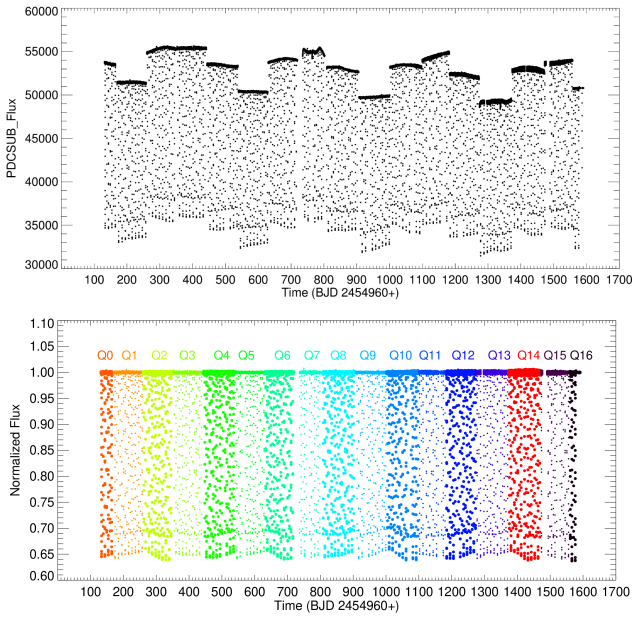

Figure 2. Kepler Q0 to Q16 observations of KIC 2306740 raw data (upper panel) and de-trended (lower panel) data. The quarters are shown in different colors.

tion was used to account for the fact that the data were obtained in long cadence by the *Kepler* satellite (see Southworth 2011). The fractional radii were fitted using their sum and ratio as these are less correlated. The orbital eccentricity e and argument of periastron ω, were fitted using the Poincaré parameters $e\cos\omega$ and $e\sin\omega$, for the same reason. Uncertainties were calculated for each fitted parameter and for each derived parameter in this study. This was done in two ways: using Monte Carlo and residual-permutation simulations (Southworth 2008). The uncertainties from the residual-permutation algorithm were found to be larger by typically a factor of 1.5 than those from the Monte Carlo algorithm, so were adopted as the final errorbars.

Simultaneous LC and RV solutions were made using the full Q0–Q16 data and the analyses are summarized in Table 4. In Fig. 3 the computed light curves are shown by solid lines. Prša et al. (2011) gave preliminary orbital parameters for 1879 *Kepler* binary systems, including KIC 2306740. They obtained a temperature ratio of 0.86, a sum of the fractional radii of 0.1374 and a $\sin i$ of 0.99919. Our analysis includes RVs as well as much more extensive LCs, so the results given in Table 4 differ from those found by Prša et al. (2011).

4. PHYSICAL PARAMETERS OF THE COMPONENTS

The physical parameters of a binary system can best be derived if it is a double-lined eclipsing binary system with an accurate light curve. Hence, the detached binary system KIC 2306740, for which the photometric and spectroscopic

Table 4. Fitted and parameters for KIC 2306740 from the JKTEBOP analysis.

Parameter	Value
Fitted parameters:	
Sum of the fractional radii	0.11102 ± 0.00019
Ratio of the radii	0.7289 ± 0.0025
Central surface brightness ratio	0.9745 ± 0.0057
Orbital inclination (°)	89.670 ± 0.073
$e\cos\omega$	0.02329 ± 0.00001
$e\sin\omega$	-0.3002 ± 0.0012
Third light	0.0918 ± 0.0079
Velocity amplitude of cool component (km s^{-1})	64.00 ± 0.28
Velocity amplitude of hot component (km s^{-1})	70.87 ± 0.23
Systemtic velocity of cool component (km s^{-1})	18.70 ± 0.02
Systemtic velocity of hot component (km s^{-1})	18.57 ± 0.02
Derived parameters:	
Fractional radius of cool component	0.06421 ± 0.00006
Fractional radius of hot component	0.04681 ± 0.00017
Light ratio	0.518 ± 0.007
Orbital eccentricity e	0.3011 ± 0.0012
Argument of periastron ω (°)	274.44 ± 0.02
Mass ratio	0.903 ± 0.004

Table 5. Astrophysical parameters of KIC 2306740. The standard 1σ errors of the last digits are given in parentheses.

Parameter	Cool Component	Hot Component
Mass ($M/M_\odot$)	1.194(8)	1.078(7)
Radius ($R/R_\odot$)	1.682(4)	1.226(5)
Temperature $\log_{10}(T_{\rm eff}/K)$	3.764(18)	3.782(17)
Luminosity $\log_{10}(L/L_\odot)$	0.449(75)	0.260(72)
Surface gravity $\log_{10}(g/{\rm cm\,s^{-2}})$	4.063(2)	4.294(4)
Bolometric magnitude (M_b)	3.61(19)	4.08(18)
Absolute magnitude (M_V)	3.69	4.09
Semi-major axis ($a/R_\odot$)	26.201(44)	

data are both of high precision, is excellent for accurate determination of its parameters. The detailed LC solution of the system indicates that the stars are well detached from their Roche lobes (see Section 3).

In this study, RVs and LCs were analysed simultaneously and the orbital parameters of the system were obtained. With the measurements given in Tables 3 and 4 we can estimate the physical parameters of the components given in Table 5.

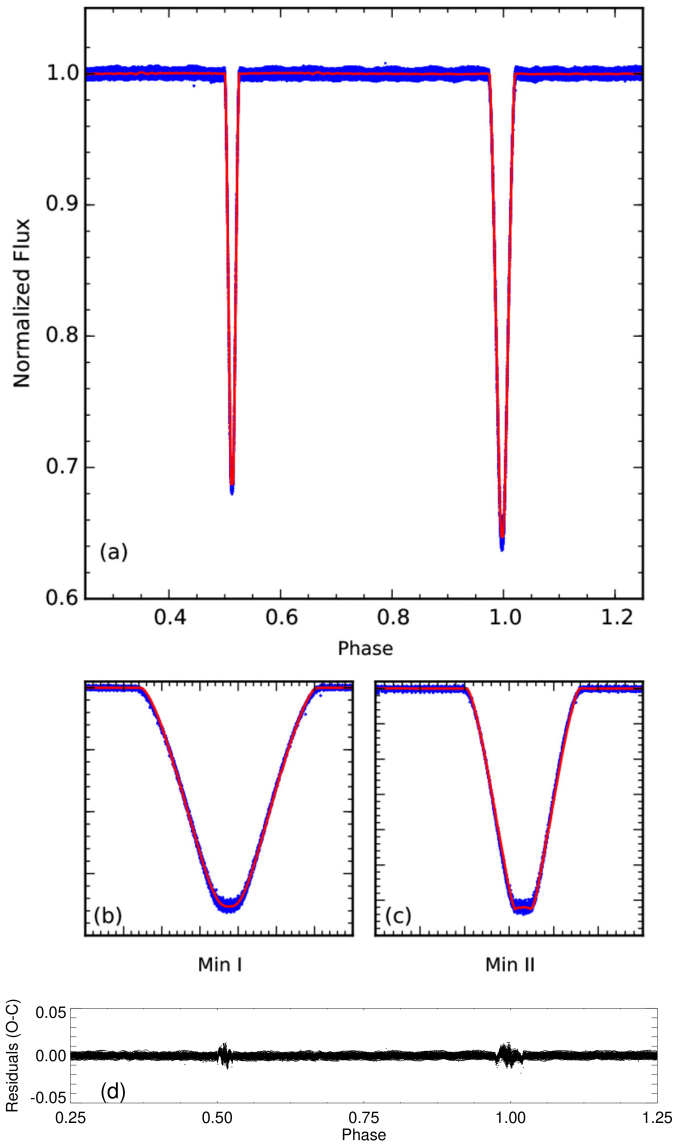

Figure 3. (a) *Kepler* full-data set observation (blue dots) and computed (red line) light curve of the system. Zoomed secondary (b) and primary (c) minima are shown to emphasize the agreement and residuals between the observed values and the corresponding LC model (d).

We have used the JKTABSDIM code [1] to estimate the physical parameters of the components, with uncertainties propagated from the LC and RV solution using a perturbation analysis. The nominal physical constants and solar properties recommended by the IAU were used (Prša, et al. 2016). All the calculated parameters of the binary system are summarized in Table 5 with their estimated errors.

[1] jktabsdim: www.astro.keele.ac.uk/ jkt/codes/jktabsdim.html

Table 6. Computed genuine frequencies, amplitudes and phase shifts of the solution. Frequencies with signal-to-noise ratios (S/N) exceeding 4 are considered as significant.

Frequency /d^{-1}		Amplitude /mmag		Phase ϕ		S/N
1.36410248	(1)	2.9497	(1)	3.6848	(1)	860
1.36287801	(1)	1.0037	(1)	1.5393	(3)	224
1.36930353	(2)	0.3028	(1)	2.9146	(8)	82
0.29110156	(4)	0.1311	(1)	5.7778	(19)	32
0.0970908	(5)	0.1103	(1)	1.9516	(25)	22

The masses of the two stars are slightly greater than solar and the radii are significantly larger. The hotter star is the less massive and has the smaller radius. This indicates that the larger star is near the end of its main-sequence lifetime. We discuss this in Section 6.

5. LIGHT VARIATION OUTSIDE ECLIPSE

Investigating of the sinusoidal brightness variation in the LC requires the extraction of the effects of binarity from the LC. After making the simultaneous LC and RV analysis, we subtracted the binary model from the observations. The residuals from the phased light variation of the binary are plotted in the Fig. 5. The oscillatory pattern can be seen clearly.

Since programs using modern light curve modeling were not perfect at representing *Kepler* data, we performed a frequency analysis on all the long cadence data obtained out-of-eclipse using the SIGSPEC (Reegen 2007) and PERIOD04 (Lenz & Breger 2005) codes, which are based on classical Fourier analysis. A signal-to-noise ratio $S/N > 4$ threshold was chosen as a criterion to consider a frequency as significant (Breger et al. 2011). We searched for significant peaks in the frequency interval from 0 to the Nyquist frequency of $25\,\mathrm{d}^{-1}$ but found no meaningful peak above $4\,\mathrm{d}^{-1}$. Fig. 4a shows the amplitude spectrum before pre-whitening of any frequency between 0 and $25\,\mathrm{d}^{-1}$. Higher amplitude peaks gather below a frequency of $5\,\mathrm{d}^{-1}$. We continued to obtain pre-whitened frequencies until the signal amplitudes fell below four times the average noise. Fig. 4b represents the spectra after pre–whitening.

Table 6 lists these genuine frequencies, their amplitudes, phases and S/Ns sorted by decreasing amplitude. Signal-to-noise ratios were computed over an interval of $5\,\mathrm{d}^{-1}$. In the top panel of Fig. 5 the agreement between 100 calculated frequencies and the observational data is plotted for almost 4 yr. The bottom panel illustrates the zoomed data of 10 d for clarity. The analysis resulted in the detection of five genuine and more than 100 combination frequencies.

What could be the mechanism that caused a change in the maximum amplitude of the KIC 2306740 system? Generally, such changes may result from stellar pulsating and/or

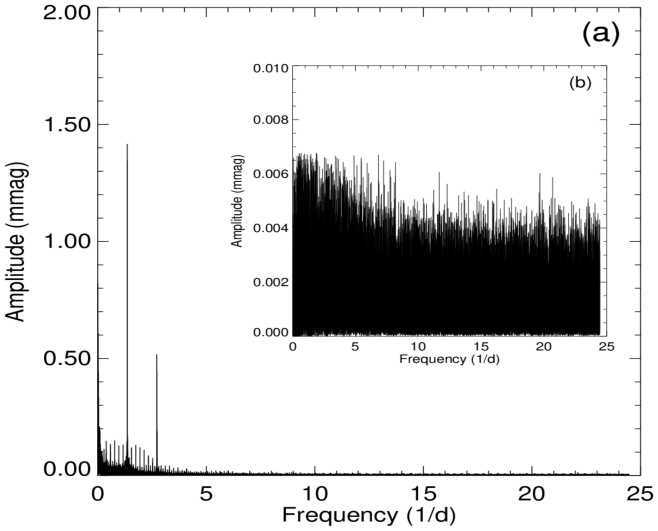

Figure 4. Amplitude A spectrum of the components before (a) and after (b) pre-whitening of all frequencies ν.

periodic changes. In binary star systems, inhomogeneous structures (e.g. stellar spots) on the surface of one or both of the component stars can cause changes in the light curve in asynchronous situations, known as rotational variability. For the frequencies obtained from the Fourier analysis of the light variation of the KIC 2306740 system (Table 6), periods of approximately 0.7 d, 3.4 d and 10.3 d were obtained. The 10.3 d period is related to the orbital period and the 3.4 d period is related to the spin period of the stars (see Section 6). The source of the 0.7 d periodicity may be γ Dor-type pulsation or spot modulations on one or both of the component(s). Besides, looking into out-of-eclipse of light variation of the system we analyzed minima phases of the light curves. There is a variation with an amplitude of 0.03 at the primary minimum and a variation with an amplitude of 0.013 at the secondary minima. However, residual data is not sufficient to estimate new frequencies.

6. RESULTS AND CONCLUSION

We have modeled the light and radial velocity curves of the well-detached binary system KIC 2306740 and determined its orbital and physical parameters (Tables 4 and 5). Solutions indicate that the more massive and cooler component of the system is more evolved than the hotter less massive component. Recently, Gaia gave a parallax of 0.6606±0.0165 mas (Gaia Collaboration 2018) for the KIC 2306740 (Gaia DR2 2051885033280089216). Using this Gaia parallax and our results we derive a distance modulus of $m_V - M_V = 11\overset{\mathrm{m}}{.}28$ and magnitudes for the components and the system of $V_1 = 14\overset{\mathrm{m}}{.}97 \pm 0.10$, $V_2 = 15\overset{\mathrm{m}}{.}50 \pm 0.12$ and $V_{\mathrm{total}} = 14\overset{\mathrm{m}}{.}50 \pm 0.11$. The new stellar parameters and reddening, reveal the distance of the system to be 1.53 kpc,

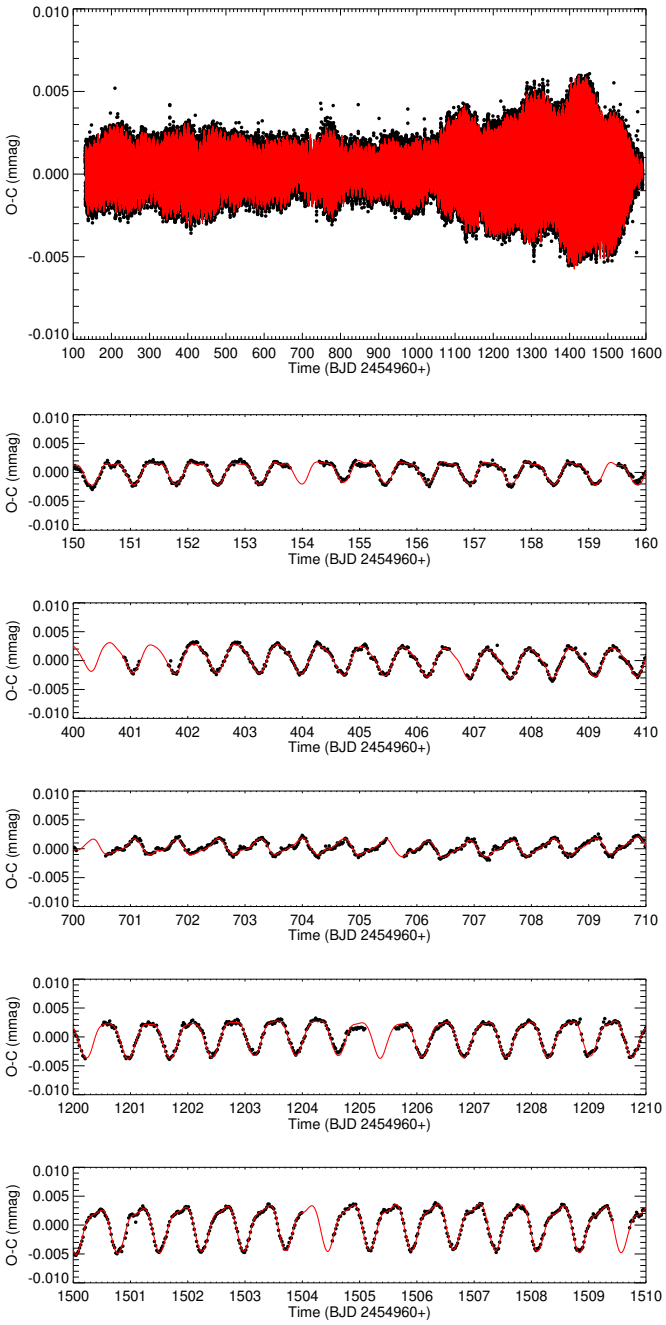

Figure 5. Part of data used in the frequency analysis (upper panel) is zoomed for different time intervals (lower panel).

which is very close to the distance obtained by Gaia as 1.51 kpc. With these results we can add the system to the list of well-determined binary stars. The maximum light shows cyclical variations.

Out-of-eclipse light variations have been obtained after eliminating the effects of binarity for the established orbit. A frequency analysis of these data revealed more than 100 fre-

quencies of which 5 are significant non-combination frequencies. The results from this study indicate that the system KIC 2306740 may contains a non-radial pulsating γ Dor type star which pulsates in high-order gravity-modes. Considering the other frequencies ($\sim$ 3.4 d, half of the spin periods) obtained, we have found that this is related to the predicted spin period of $\sim$ 6.8 days (see Fig. 6).

we have found that the component stars are related to the spin periods ($\sim$ 6.8 d) obtained (see Fig. 6c). This tells us that at least one of the components has changed due to inhomogeneous structures on its surface. This also tells us that spot modulation is a possible explanation for the variation at the maxima phases, instead of pulsations. Using the parameters we have obtained (Table 5) show that the components of binary system KIC 2306740 is outside or on the edge of the instability zone in the HR diagram. Therefore, the light variation seen in this system is likely caused by spot modulation.

We use this system to test the theory of modeling stellar interiors by comparing with its the observational properties. Models were constructed with the EV code (Eggleton & Kiseleva-Eggleton 2002) and its much more powerful TWIN variant (Yakut & Eggleton 2005; Eggleton 2006; Eggleton 2010), both of which are based on the Cambridge STARS code (Eggleton 1971, 1972, 1973; Pols et al. 1995). In single-star evolution, as in the STARS code, the effects of rotation and magnetic dynamo activity on mass loss and the proximity of the companion are usually not considered. TWIN allows various non-conservative processes to be applied to the primary component of a binary system. *Both* components are modeled *simultaneously* so that the effects of tidal friction, magnetic dynamo activity, and hence mass loss, can be incuded according to a self-consistent prescription. Mass loss carries off angular momentum by way of magnetic braking.

In the case of non-conservative evolution it is hard to find initial parameters that would lead to the current binary system (see Eggleton & Yakut 2017). However we can reasonably assume that the initial masses were larger than now. Table 7 gives parameters for a model that is slightly metal-rich ($Z = 0.03$) compared to the Sun. This metallicity gives a somewhat better fit than solar.

After some experimentation, we evolved a pair of stars with initial masses of 1.21 and 1.08 $M_\odot$, each with spin periods of 3.0 d, an eccentricity of 0.34 and an orbital period of 10.30 d. We expect the orbital period to decrease as the orbit circularizes and as angular momentum is lost by wind mass loss and magnetic braking. However the period also *increases* on account of the orbit acquiring some angular momentum from the spins of the stars by tides. The particular model of the non-conservative processes in the TWIN code led the system to evolve to roughly the observed masses and radii in about 5.1 Gyr.

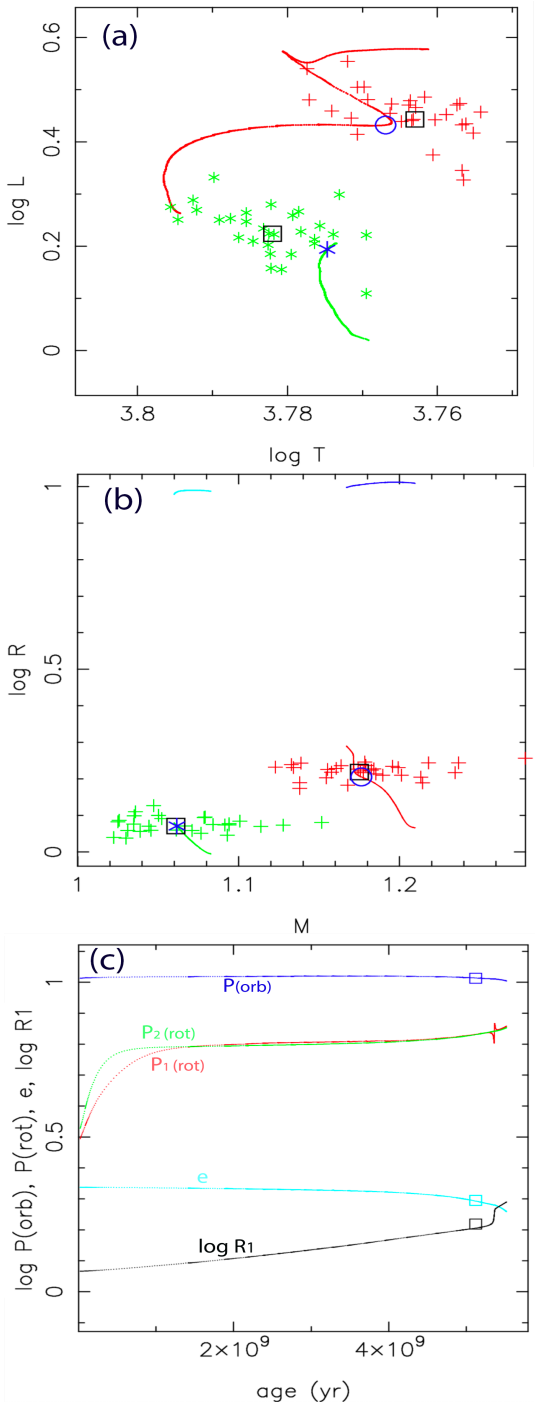

Figure 6. Evolutionary tracks for our best model of KIC 2306740. Our data for KIC 2306740 are shown as squares. Panel (a) shows the evolution in the $\log L - \log T$ plane. The primary's and secondary's tracks are shown with red and green lines, respectively. The extent of the red and green pluses represent roughly the observational uncertainties. Panel (b) shows the primary's radii (red) and lobe radii (dark blue) and secondary's radii (green) and lobe-radii (light blue) as a function of mass. Panel (c) shows the time-evolution of orbital period (dark blue), spin period of the primary (red) and the secondary (green), eccentricity (light blue) and radius of primary (black).

Table 7. An Evolutionary Model for KIC 2306740.

Parameter	Zero age	Age 5.12 Gyr	Observed
P/d	10.30	10.32	10.307
e	0.337	0.293	0.301
$M_1/M_\odot$	1.210	1.176	1.194
$\log_{10}(R_1/R_\odot)$	0.058	0.206	0.225
$\log_{10}(L_1/L_\odot)$	0.208	0.432	0.449
$\log_{10}(T_1/\mathrm{K})$	3.785	3.767	3.764
$M_2/M_\odot$	1.083	1.062	1.078
$\log_{10}(R_2/R_\odot)$	–0.013	0.071	0.088
$\log_{10}(L_2/L_\odot)$	–0.005	0.194	0.260
$\log_{10}(T_2/\mathrm{K})$	3.767	3.775	3.782

Fig. 6 shows evolutionary tracks in three planes, (a) the $\log L - \log T$ plane or theoretical HR diagram, (b) the $\log R - \log M$ plane and (c) the $\log P$ − age plane for both spin and orbital periods periods together with eccentricity e and $\log R_1$. Our data for KIC 2306740 are represented by squares in panels (a) and (b). Each square is surrounded by a cloud of plusses generated by a Gaussian random number generator to illustrate the extent of the standard errors in the basic observational data (K_1, K_2, T_1, ...). The evolutionary tracks for the more massive star (*1) are red and for less massive star (*2) green. A blue circle approximately marks the best fit to $*1$ and a blue asterisk the coeval point for $*2$. Panel (b) shows the Roche lobe radii as well as the actual radii. Neither star is within a factor of 5 of its Roche radius. Panel (c) shows the spin periods in red and green. Both were started arbitrarily at 3 d and rather rapidly evolved to about 6 d before reaching a plateau. During this fairly rapid initial spin-down the components lost about 0.03 and 0.02 $M_\odot$ of their masses. The logarithm of the orbital period is dark blue, the eccentrcity is light blue and the radius of star 1 is black. Table 7 shows the evolutionary changes in some major variables. Our overall conclusion from Fig. 6 is that the fit of to the theoretical model is acceptable at a 1σ level but it would be better if the model temperatures matched more closely those observed.

We are very grateful to an anonymous referee for comments and helpful, constructive suggestions, which helped us to improve the paper. The authors gratefully acknowledge the numerous people who have helped the NASA *Kepler* mission possible. This study was supported by the Turkish Scientific and Research Council (TÜBİTAK 117F188). DK is grateful to the Astronomy Department of the University of Geneva (Geneva Observatory) for the kind hospitality during her visit and gratefully acknowledge the support provided by the TÜBİTAK-BİDEB 2211-C and 2214-A scholarships. CAT thanks Churchill College for his Fellowship. KY would like to acknowledge the contribution of COST (European Cooperation in Science and Technology) Action CA15117 and CA16104.

Facilities: Kepler, William Herschel Telescope (WHT)

Software: TODCOR (Zucker & Mazeh 1994) , PAMELA (Marsh 1989), SIGSPEC (Reegen 2007), PERIOD04 (Lenz & Breger 2005), TWIN (Yakut & Eggleton 2005; Eggleton 2006; Eggleton 2010), CAMBRIDGE STARS CODE (Eggleton 1971, 1972, 1973; Pols et al. 1995)

REFERENCES

Aerts C., Harmanec P., 2004, ASPC, 318, 325
Aerts C., Christensen-Dalsgaard J., Kurtz D. W., 2010, Asteroseismology (Springer)
Aerts C., 2013, EAS, 64, 323. doi:10.1051/eas/1364045
Armstrong D. J., Gómez Maqueo Chew Y., Faedi F., Pollacco D., 2014, MNRAS, 437, 3473
Borucki W. J., et al., 2010, Sci, 327, 977
Breger M., 2005, ASPC, 333, 138
Breger M., et al., 2011, MNRAS, 479
Brown T. M., Latham D. W., Everett M. E., Esquerdo G. A., 2011, AJ, 142, 112
Çokluk K. A., Koçak D., Içli T., Karaköse S., Üstündağ S., Yakut K., 2019, MNRAS, 488, 4520
Eggleton, P. P., & Kiseleva-Eggleton, L. 2002, ApJ, 575, 461
Eggleton P. P., 1971, MNRAS, 151, 351
Eggleton P. P., 1972, MNRAS, 156, 361
Eggleton P. P., 1973, MNRAS, 163, 279
Eggleton P., 2006, Evolutionary Processes in Binary and Multiple Stars, Cambridge University Press
Eggleton P. P., 2010, NewAR, 54, 45
Eggleton P. P., Yakut K., 2017, MNRAS, 468, 3533
Gaia Collaboration, 2018, yCat, I/345
Gimenez A., Garcia-Pelayo J. M., 1983, Ap&SS, 92, 203
Gilliland R. L., et al., 2010, PASP, 122, 131
Huber D., 2015, ASSL, 169, ASSL..408
Jenkins J. M., et al., 2010, ApJ, 713, L87
Johnston C., et al., 2019, MNRAS, 482, 1231
Kjurkchieva D., Vasileva D., Atanasova T., 2017, AJ, 154, 105
Koch D. G., et al., 2010, ApJ, 713, L79
Lenz, P., Breger, M., 2005, Commun. Asteroseismol. 146, 53
Maceroni C., et al., 2014, A&A, 563, A59
Marsh T. R., 1989, PASP, 101, 1032

Maxted P. F. L., et al., 2020, MNRAS.tmp, doi:10.1093/mnras/staa1662
Murphy S. J., Moe M., Kurtz D. W., Bedding T. R., Shibahashi H., Boffin H. M. J., 2018, MNRAS, 474, 4322
Pols O. R., Tout C. A., Eggleton P. P., Han Z., 1995, MNRAS, 274, 964
Prša, A., Zwitter, T., 2005, ApJ, 628, 426
Prša A., et al., 2011, AJ, 141, 83
Prša A., et al., 2016, AJ, 152, 41
Qian S.-B., Li L.-J., He J.-J., Zhang J., Zhu L.-Y., Han Z.-T., 2018, MNRAS, 475, 478
Reed M. D., Brondel B. J., Kawaler S. D., 2005, ApJ, 634, 602
Reegen P., 2007, A&A, 467, 1353
Southworth J., 2008, MNRAS, 386, 1644
Southworth J., 2011, MNRAS, 417, 2166
Southworth J., 2013, A&A, 557, A119
Southworth J., Maxted P. F. L., Smalley B., 2004, MNRAS, 351, 1277
Southworth J., Bowman D. M., Tkachenko A., Pavlovski K., 2020, MNRAS, 497, L19. doi:10.1093/mnrasl/slaa091
Smalley, B. and Smith, K. C. and Dworetsky, M. M., 2001, UCLSYN Userguide
Smith, K. C., 1992, PhD Thesis, University of London
Sing D. K., 2010, A&A, 510, A21
Tonry J., Davis M., 1979, AJ, 84, 1511
Torres G., Andersen J., Giménez A., 2010, A&ARv, 18, 67. doi:10.1007/s00159-009-0025-1
Welsh W. F., et al., 2011, ApJS, 197, 4
Wilson R. E., 1979, ApJ, 234, 1054
Wilson, R.E., Devinney, E.J., 1971, ApJ, 166, 605
Wood P. R., Olivier E. A., Kawaler S. D., 2004, ApJ, 604, 800
Yakut K., Eggleton P. P., 2005, ApJ, 629, 1055
Yakut K., Aerts C., Morel T., 2007, A&A, 467, 647
Yakut K., Eggleton P. P., Kalomeni B., Tout C. A., Eldridge J. J., 2015, MNRAS, 453, 2937
Zacharias N., Monet D. G., Levine S. E., Urban S. E., Gaume R., Wycoff G. L., 2005, yCat, 1297, 0
Zahn J.-P., 1975, A&A, 41, 329
Zucker S., Mazeh T., 1994, ApJ, 420, 806